FIELD EMISSION STUDIES IN SUPERCONDUCTING CAVITIES *

H. Padamsee, C. Reece, R. Noer†, W. Hartung, E. Frick and R. Kahn

Laboratory of Nuclear Studies, Cornell University, Ithaca, NY 14853

Abstract

Current experience with 1-cell superconducting (sc) cavities prepared from the highest thermal conductivity material by the best available techniques shows that the dominant limitation to achieving high accelerating gradients is field emission loading. Emitters are studied using high purity Nb single-cell, 1500 MHz elliptical cavities equipped with a new thermometry system (684 sensors) capable of scanning the entire surface of the cavity within a few seconds. Operation of this rapid temperature mapping system in superfluid He is a necessary advance for high field study over customarily used subcooled He diagnostics. Emitter properties are determined by comparison with calculations of field emitted electron trajectories and their associated power deposition.

Introduction

With the universal adoption of spherical and elliptical cavities for velocity of light structures, as well as the shift to high thermal conductivity niobium, the old problems of multipacting and thermal breakdown in sc cavities have been overcome. These advances have given a firm basis for the application of sc cavities to high energy electron storage rings and recirculating electron linacs for which gradients of 5 MeV/m can be effectively utilized.[1] Higher gradients would open the possibility of future application to TeV-scale colliding linacs and to upgrading machines now being built or contemplated.[2] The dominant limitation to achieving higher gradients in sc cavities that faces us today is field emission (FE) loading.

Direct evidence for localized FE in rf cavities has emerged from temperature maps, i.e. detailed measurements of wall temperature increases caused by impinging electrons.[3] Computer calculations of electron trajectories and impact energies resulting from known cavity fields show that the observed heating patterns are consistent with emission sources between 10^{-6} and 10^{-14} cm^2 in area and field enhancement factors β from 100 to 750.[4]

Only a few emitters have been studied by this potentially powerful method. One of the reasons for the scarcity of data is that the temperature mapping system used is slow, being based on rotating a single arm bearing an array of thermometers. Typically an hour of data taking is necessary at a single field level. An additional disadvantage is the inability to capture data on the time dependent behavior of unstable emitters.

To improve our understanding of field emission behavior in rf fields from cold surfaces there is a need to substantially augment the data available on the density of emitters, on their Fowler-Nordheim (FN) and processing characteristics. Very useful information can also be gained from a study of the distribution of emitter sites and from the capability to localize individual sites. For example, it is interesting to determine whether particular cavity treatments produce or reduce sites or merely modify the emission strength of existing sites.

High Speed Superfluid Thermometry

To obtain a map in a few seconds, we have chosen to cover the outer cavity wall with a large number of thermometers at fixed locations, rather than mechanically moving a smaller array over the surface. For high field studies, operation in superfluid helium is necessary. In subcooled He temperature diagnostics systems used up to now, the low heat transfer coefficient of subcooled He, as well as the higher temperature (>2.2 K) can force the rf surface temperature to increase unstably at high fields due to BCS losses at 1500 MHz. Heat flow calculations and experiments show that the spatial resolution of superfluid thermometry is increased by a factor of 2.5.[5]

Substantial improvements in thermometry sensitivity are needed for carrying out measurements in superfluid due to the high heat transfer between the Nb wall and the cooling bath. For example, at heat flux densities of 1 mw/cm^2, the theoretical temperature rise at the outer wall drops from 130 mK in subcooled He[6] at 2.2 K to 7 mK in superfluid at 1.5 K, assuming the Kapitza resistance of unannealed reactor grade Nb. Lower temperature increments are expected with annealed Nb.[7]

684 thermometers developed for this system have been mass-produced and designed to have good sensitivity. One key ingredient has been the ability to isolate the heat sensitive element of the thermometer from the superfluid. Carbon resistors are embedded in a G-10 expoxy housing and sealed with Stycast epoxy, known to be impervious to superfluid He. Thin manganin leads are used to reduce heat transfer to the bath via sensor leads. Another factor essential to high sensitivity has been to establish intimate contact between the sensor and the outer surface of the cavity. The surface of the assembly is ground plane until the carbon element is exposed and subsequently electrically insulated by several layers of GE-varnish. ApiezonN grease is applied between the thermometer and cavity surface and the assembly is pressed against the cavity wall with a Be-Cu spring loaded contact pin. The pins are captured inside holes machined in G-10 boards which are contoured to follow the cavity shape. Only a fraction (efficiency) of the differential between the cavity wall and bath temperatures is measured by thermometers immersed in superfluid. As in the past,[5] the efficiency of a few thermometers has been tested in a separate calibration apparatus and found to be approximately 30%. Wiring

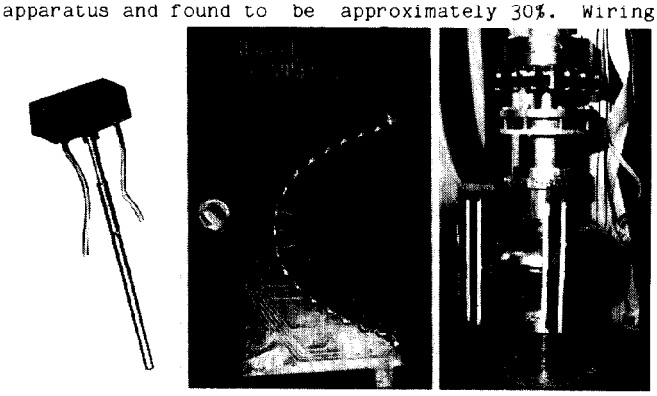

Figure 1. Single cell 1500 Mhz cavity with printed circuit boards bearing 19 thermometers sensitive in superfluid Helium. An individual thermometer assembly is shown on the left. Boards are placed at 10° azimuthal intervals.

*Supported by the NSF with supplementary support from the US-Japan Collaboration.

†Present address: Carleton College, Northfield, MN.

CH2387-9/87/0000-1824 $1.00 © IEEE

for such a large array is made compact by printed circuitry over the surface of the holder boards (Fig. 1). Our temperature mapping electronics with room temperature multiplexers and matrix wiring scheme, which has been used previously on 5-cell cavities, has been expanded to cover the larger number of resistors, and a computerized read-out system has been installed.

Typical Temperature Maps

Thermometers are calibrated against the bath temperature between 2.5 and 1.4 K. To acquire a temperature map at a certain field, the resistors are scanned once with the rf turned off, and a second time with the rf on. The bath temperature is also measured at the start and stop of each scan to aid in correcting bath drifts. The entire data acquisition process is complete within 15 secs after which the resultant map can be displayed in a variety of ways with available software. A typical 3-D display showing heating due to field emission and a defect is shown in Fig. 2. Maps can be taken in rapid succession at increasing field levels, so that field level dependent phenomena can be studied. For detailed analysis, the data is transferred off-line to a main-frame VAX computer. Fig. 3a and 3b show superposed longitudinal temperature profiles along a fixed meridian taken at several

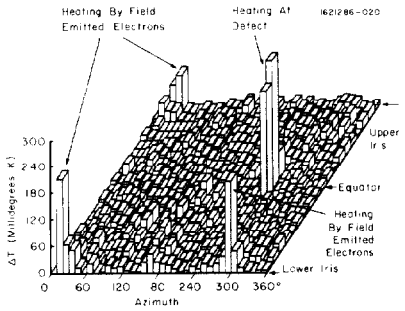

Figure 2. A typical high speed superfluid helium temperature map showing heating by field emitted electrons and at a defect on the equational weld. Surface E_{peak} = 15 Mv/m.

increasing field levels for (a)emitter and (b)defect heating. The temperature increases can be plotted in a FN format for field emission heating, or vs. E^2 for defect heating.

To the best of our knowledge, this is the first time that local heating can be studied as a detail function of field level, made possible by the rapidity of the mapping system.

Heating at Defects

In one experiment we encountered a defect that exhibits a sc-nc transition, and fortuitously, provides an in-situ calibration of the thermometer response. While sc below 275 Oe, the defect becomes nc above, and the field level in the cavity drops to 225 Oe but the cavity does not breakdown. Rf data provide a measurement of the total dissipated power while the defect is nc. By subtracting the dissipated power at 225 Oe while the defect was sc, it is determined that the defect alone is dissipating 90 mw of power in the nc state at 225 Oe and the maximum ΔT is ~120 mK (see Fig. 3b). Assuming a surface resistance typical for normal state Nb, (10^{-2} ohms), this defect is estimated to be 250 microns in diameter. Subsequent inspection of the cavity interior with a Questar™ telescope showed the defect to be located at the overlap of the start and stop regions of the equator e-beam weld. Judging by the smallest temperature signals that we can resolve from the noise (5-10 mK), we expect to be able to detect nc defects as small as

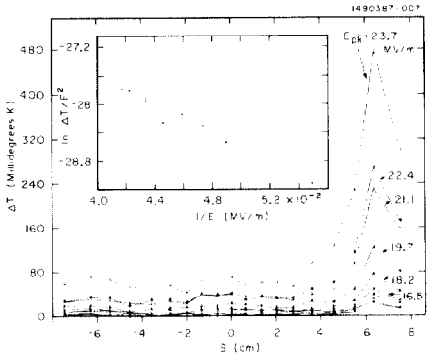

Figure 3a. Experimental temperature map due to FE heating from one emitter at several field levels. The inset shows the peak temperature data in a FN plot. Error bars are standard deviation from 3 consecutive measurements.

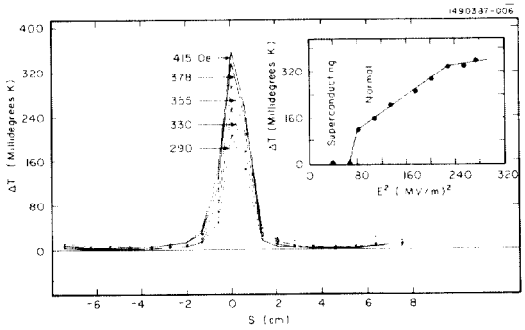

Figure 3b. Experimental temperature maps due to a weak superconducting defect at various field levels. The inset shows the sc to nc transition and the linear behavior of ΔT vs. E^2 after the transition.

60 microns and even smaller defects at higher fields.

Unstable Emitters

Another major benefit derived from high-speed mapping is the study of time dependent behavior of individual emitter heating. On occasion, we have found some emitters to switch[8] from a low into a high emissive state. A correlated jump in the current collected by an rf antenna in the cavity is observed. Increased dissipation triggered by such switches also cause the field level to drop, but without any accompanied decrease in the emissivity of the switched site. Figure 4 (center) shows one example of a scan

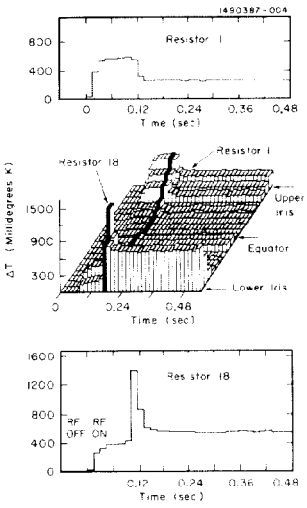

Figure 4. Time dependent temperature map showing switching behavior of emitter on lower iris. Emission from then upper iris is reduced when the field level drops due to increased emission from the lower iris.

at 30 msecs intervals for the heating profile at a fixed azimuth; the upper and lower graphs depict the time dependence at two thermometers near the irises. Heating due to an emitter located near the upper iris shows the cavity fill time and the equilibrium emission at a stable field level. When the emitter at the lower iris abruptly increases emission, the field level drops, lowering heating from the upper emitter. The lower emitter maintains higher emission in spite of the field drop.

Comparison with Trajectory Calculations

For a thorough analysis of field emission heating, a parallel effort is necessary to calculate trajectories of electrons emanating from possible sites, and to compute the power density at electron impact. Following similar previous efforts,[3] we show in Fig. 5 calculated trajectories at one field level for an emitter near the peak field region. We also show temperature profiles for several field levels calculated by smearing the deposited power to simulate heat flow through the Nb wall. A full-width at half- maximum of 1.6 cm is chosen corresponding to observed temperature profile widths. The loss distribution is peaked near the emitter, allowing a quick estimate of the location. The evolution of the calculated temperature profiles with field level should be compared with observed profiles as shown in Fig. 3a.

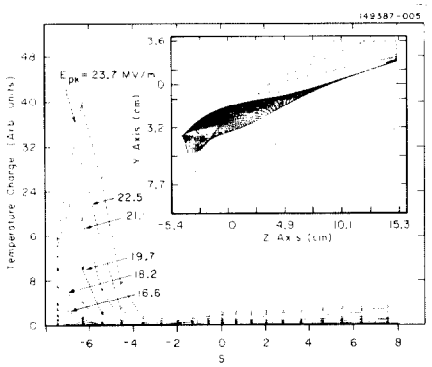

Figure 5. Calculated temperature maps from field emission heating at various field levels. These should be compared with observed maps in Fig. 3a. The inset shows trajectories for one rf period at the highest field level.

Variation of Emitter Landscape With Cavity Exposure

In one series of tests, we studied the effect on the temperature maps due to various exposures. With this cavity it was only possible to reach 17 - 20 Mv/m peak electric field before emitter switching heavily loaded the cavity. In the first emission two tests, after allowing heavy field (50 - 100 watts of dissipated power during emission), we merely warmed up the cavity without physically moving or disturbing it. On the following cold test, we noticed that the predominant emission area was quiet (300° in Fig. 6a). This emitter was previously responsible for occasional breakdown from the impinging current. Slightly higher field levels could be reached. Figure 6 shows the maps before and after warming. Continuing this series, we re-tested the cavity and took temperature maps each time after different slow exposures of gas at room temperature: 0.1 torr of He, 0.1 torr filtered N_2, 760 torr filtered N_2, 760 torr filtered O_2, and 760 torr filtered air. At the highest field level before switching, the emitter landscape showed no gross changes, except for a slight increase in the last exposure. We conclude that controlled exposure does not affect emitter properties up to 20 Mv/m, confirming similar previous observations.[9]

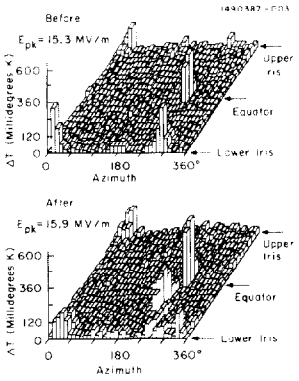

Figure 6. Temperature maps before (Ep = 15.3 Mv/m) and after (Ep = 15.9 Mv/m) warming cavity to room temperature. Emission at 300° is substantially reduced. An additional weak sc defect becomes nc at 15.9 Mv/m.

Conclusions

A program to further the understanding of FE behavior in SRF cavities has been started. High speed superfluid thermometry has been developed. With this tool, we plan to study the statistics and properties of emitters as we vary the surface treatment. Techniques such as high temperature treatment and high power He processing, which are expected to have a beneficial effect on FE, will merit extensive exploration.

Acknowledgements

We are grateful to our colleagues at Cornell, CERN and University of Wuppertal for many fruitful discussions. We also are indebted to G. Mueller (Wuppertal) for calibrating our thermometers.

References

[1] H. Padamsee, "Status and Issues of Superconducting RF Technology", This conference.

[2] R. Sundelin, "High Gradient Superconducting RF", This conference.

[3] Ph. Bernard et. al., "First Results on a Superconducting RF-Test Cavity for LEP", Proc. of the 11th Intn'l. Conf. on High Energy Accelerators, 878 (1980).

[4] W. Weingarten, "Electron Loading", Proc. of the Second Workshop on RF Superconductivity, CERN p. 551 (1984).

[5] P. Kneisel, G. Mueller and C. Reece, "Investigation of the Surface Resistance of Superconducting Niobium Using Thermometry in Superfluid Helium", 1986 Applied Superconductivity Conference.

[6] R. Romyn and W. Weingarten, "Calibration of the scanning Thermometer Resistor System for a Superconducting LEP Cavity" CERN/EF/RF 81-4 (1981)

[7] K. Mittag, Cryogenics 13, 94 (1973).

[8] K.H. Bayliss and R.V. Latham, "An Analysis of Field-induced Hot-electron Emission from Metal-insulator Microstructures on Broad-area High-voltage Electrodes", Proc. R. Soc. Lond. A 403, 285 (1986).

[9] D. Bloess et. al., "Recent Results from Superconducting 350 Mhz Single cell cavities", CERN/EF/RF 85-2 (1985).